Improving the results of the fractal model of geochemical Mineralization Probability Index Using the Gray Wolf Algorithm on the Stream Sediments Data of Sarduiyeh-Baft Area

Kamran Mostafaei[1]*, Mohammad Kianpour[2], Mahyar Yousefi[3], and Meisam Saleki[2]

1. Department of Mining, Faculty of Engineering, University of Kurdistan, Sanandaj, Iran
2. School of Materials and Mineral Resources Engineering, Engineering Campus, Universiti Sains Malaysia (USM)
3. Faculty of Engineering, Malayer University, Malayer, Iran

Article Info	Abstract
	Discrimination of geochemical anomalies from background is a challenge in that elemental dispersion patterns are affected by a variety of geological factors, which vary from one to another area. While statistical and fractal methods are commonly employed for anomaly detection, they struggle with selecting optimal thresholds. This study proposes the Grey Wolf Optimizer (GWO) algorithm as a novel approach for identifying the optimal boundary between anomalies and background. Stream sediment geochemical data from a copper-mineralized area of the Sarduiyeh-Baft sheets in southeast Iran were utilized for analysis. The Geochemical Mineralization Probability Index (GMPI) was first calculated for Cu-Au, Mo-As, Pb-Zn, and porphyry distributions. Subsequently, fractal methods were used to identify anomalous populations within each GMPI. The GWO algorithm was then applied to these distributions to determine the optimal thresholds. Risk analysis, calculated as the ratio of covered copper occurrences to the covered area, revealed superior reliability for the GWO-derived limit compared to those obtained using fractal methods. For porphyry GMPI values, while the fractal reliability indices are 0.127, 0.44, and 0.5, the GWO limit achieved a value of 0.66. Risk analysis for Cu-Au distribution also caused more desired result for GWO limit rather that fractal ones. This demonstrates the enhanced performance and superior reliability of the GWO algorithm for optimizing anomaly detection thresholds in GMPI data.

1. Introduction

Mineral exploration is carried out using a combination of different methods and techniques. The choice of methods and techniques depends on the goal of the study and the conditions of the studied area such as geology, topography, type of mineralization, etc. [1,2]. While stream sediments, as a substantial geochemical investigation, are one of the most important steps in the exploration of metal deposits, the definition of an appropriate boundary between anomaly and background has remained challenging yet [3-7]. It has become more important and requires more attention to select an appropriate approach to separate anomaly from background. Accordingly, scientists have done a lot of research to solve this dilemma by obtaining

different characteristics of geochemical data such as statistical parameters and their spatial variability [8-10]. For example, classical statistical methods are widely used to identify anomalies and background values, but they impose some assumptions on the data, such as a normal distribution or removing outlier data, which may not lead to the desired results [11-13]. A number of proposed techniques have been made and developed to overcome the problems associated with the classical statistical framework [14-19]. Following includes, but not limit, some efforts in this regard:

Using multi-fractal method for geochemical; anomaly separation in the copper-molybdenum

✉ Corresponding author: K.mostafaei@gmail.com (K. Mostafaei)

porphyry deposit of Kahang [20], utilizing fractal modeling and staged factor analysis for Cr and Fe mineralization in Balvard, SE Iran [21], combination and comparison of U-spatial and C-A fractal models for anomaly detection in Varzeghan, Iran [22], separation of geophysical anomaly by fractal methods [23], geochemical anomaly detection by novel genetic K-means clustering algorithm [24], using a hybrid technique for anomaly recognition in geochemical exploration, Dehsalm, Iran [25], improving geochemical prospectivity mapping using power spectrum-area fractal modeling [26], determination of Mo and Au distribution variances in Iranian copper porphyry deposits by the fractal methods [27], and detecting REEs anomalies using fusion fractal-wavelet model in Tarom metallogenic zone, Iran [28]. In addition, the neural network methods have been used for anomaly separation [29-33].

The principal focus of this research is to reduce errors in geochemical data analysis to make it more consistent with mineralization facts. The GMPI, as an ideal methodology, tries to settle deficiencies [34]. The GMPI focuses on a precise anomaly detection and seeks to reduce the statistical error level in stream sediment analysis as much as possible. It has been the objective of countless studies that led to outstanding results [35-39].

Metaheuristic algorithm are increasingly applicable to a wide range of scientific problems, including geological ones. These algorithms mimic strategies that living organisms use to fulfill their needs, such as hunting, nesting, etc. They can solve complex problems by gaining fast and logical solutions [40,41]. Swarm intelligence algorithms rely on distinctive features such as self-organization, parallel processing, and high flexibility to estimate different parameters in robot control, transportation, communication networks, etc. [42-44]. Gray Wolf Optimizer (GWO) algorithm has been applied to geo-related problems: geoelectrical data inversion [45], solving engineering design problems [46], network and wireless [47], feature selection [48], lidar signal noise reduction [49], and mineral prospectivity mapping [50].

In the mentioned previous researches with fractal methods, geochemical data were divided into some groups by different limits that we should select the anomaly group by determining anomaly limits. This paper proposes a novel approach to the elimination of expert opinion in the separation of geochemical anomalies. Also, a new application of swarm intelligence in geochemical analysis is presented in this research.

The objective of the study is to conduct a geochemical analysis leading to a binary map that only contains anomalous and non-anomalous zones within the Sarduiyeh-Baft area, which has a high potential for copper porphyry mineralization in Iran. According to the prepared GMPI spatial distribution for Cu-Au, Mo-As, Pb-Zn, and porphyry index through of the area, separation limits between statistical populations were measured by fractal analysis. Finally, the GWO algorithm was applied to obtain the optimized value among the GMPI values using derived fractal limits. Validation and risk analysis of our findings confirm that GWOs actions were in line with the research objective.

2. The study area and data

The case study is located in Kerman Province, Iran. The study area includes parts of two 100,000 geological sheets called Sarduiyeh and Baft (provided by the Geological Survey of Iran). This area is a part of the Urumieh-Dokhtar belt and (Figure 1). The Urumieh-Dokhtar volcanic belt is a result of the subduction of the Arabian plate beneath central Iran during the Alpine orogeny [51-53].

Regionally speaking, volcanic and pyroclastic rocks belong to the Eocene epoch and mostly consist of andesite, basalt, rhyolite flows, Algoma, and different tuff types through the study area [54]. These units got altered by abysmal Oligocene intrusive body leading to metamorphism and mineralization. During intrusion phase, magmatic segregation occurred within intrusive bodies and their composition transferred to quartz-diorites and quartz-monzonite from a granodiorite origin. The final derived phase was enormously affected by rich-silicate and ore-bearing solutions caused to the extension of silicic veins and veinlets. The area is in a tectonically active region and most fractures result of fault activation and dominant dykes are micro-diorite ones that occasionally reach 1 kilometer in length [51,55].

There are four main lithological groups in this area, based on the geological map of the study area, including intrusive rocks, volcanic rocks, sedimentary rocks, and colored mélange (Figure 2). There are many copper porphyry deposits in this volcanic belt, including 37 known Cu porphyry deposits in the study area, which were used for validation. The porphyry occurrence in the study area is related to subduction of Arabian and Central Iran plates [51,52]. The main host rocks are quartz-monzonite, monzonite, granodiorite and quartz-

diorites where mineralization is mainly occurred at the contact of these rock types with volcanic rocks [36,52]. Hydrothermal alteration, including argillic, phyllic and iron-oxide alteration, is present at the surface of most of the copper porphyry deposits that can be detected by remote sensing [57,58]. Gold, copper and molybdenum are the main elements in these porphyry deposits [34,59]. 1478 stream sediment data were used for geochemical analysis to generate the GMPI maps [9]. It is noteworthy that the samples were subjected to chemical analysis for 49 elements using the ICP-MS methods by geological survey of Iran.
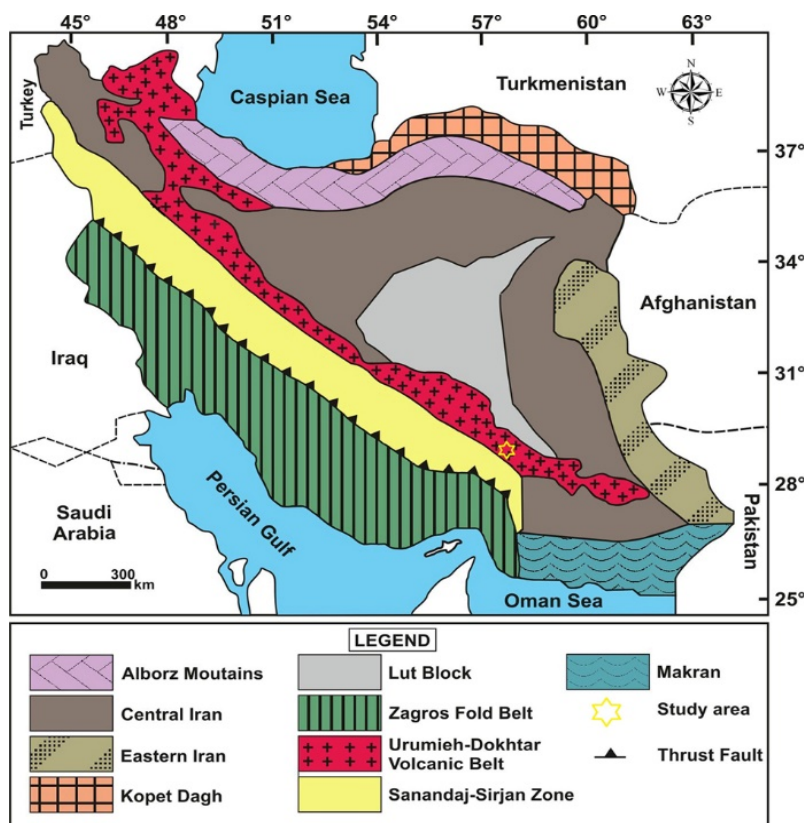

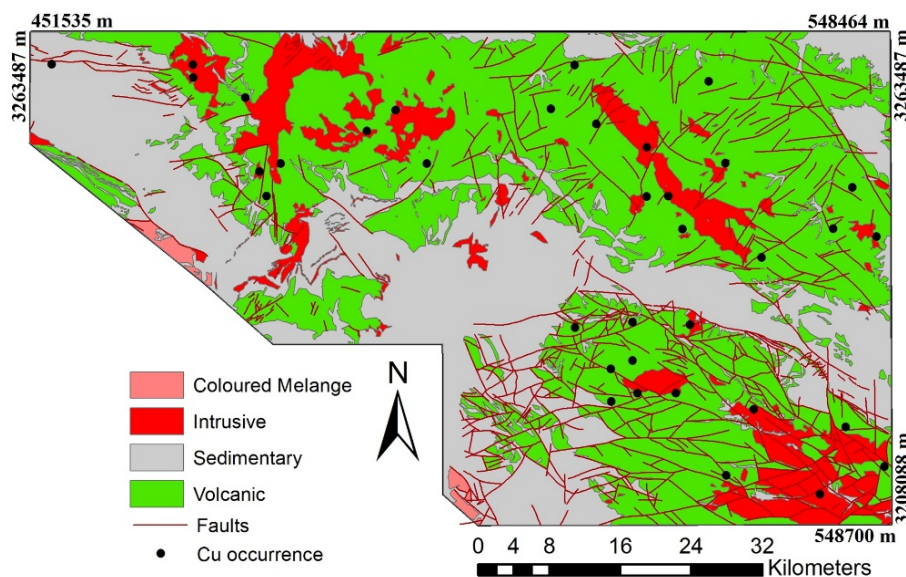**Figure 1. Structural map of iron [60] and study area position**

Figure 2. A simplified geological map of the study area was prepared by the Geological Survey of Iran [61]

3. Methods

3.1. Geochemical Mineralization Probability Index (GMPI)

Anomaly detection is the primary objective of geochemical data analysis. The GMPI is a new method that was developed by Yousefi et al., 2012 to improve the production of the geochemical evidence maps for stream sediment samples [34]. This method is a weighting method that can be mapped and can be used as the main layer in Mineral Prospectivity Mapping (MPM) studies for mineral exploration.

In the analysis of geochemical data, factor analysis is usually performed, factor scores are calculated, and then geochemical maps are produced based on the scores that show the probability of mineralization upstream of each sample [62]. The GMPI method is the application of the logistic function on the factor scores obtained from stepwise factor analysis, which is referred to as fuzzy weight. To calculate the GMPI values equation 1 is used [34].

$$GMPI = \frac{e^{Fs}}{1 + e^{Fs}} \tag{1}$$

Where Fs is each sample's factor score per indicator component from factor analysis.

3.2. Gray Wolf Optimization (GWO) Algorithm

The GWO algorithm simulates the social behavior of gray wolves in nature and their hunting method [63,43]. This meta-heuristic algorithm has developed according to swarm intelligence and includes the following stages: a) Observing, tracking, and chasing prey, b) approaching and surrounding prey leading to prey's confusion and stops moving, and c) attacking prey.

In this algorithm, wolves are divided into four groups: alpha or leader, beta, delta, and omega wolves. The main directors of the algorithm are alpha wolves. Beta and delta assist alpha wolves and omega wolves follow others [43]. In the first step of the algorithm, gray wolves surround the prey. Following describes the mathematical model for surrounding prey:

$$\vec{D} = |\vec{C}.\vec{X}_P(t) - \vec{X}_{(t)}| \tag{2}$$

$$\vec{X}_{(t+1)} = \vec{X}_P(t) - \vec{A}.\vec{D} \tag{3}$$

In the aforementioned equations, $X_{(t)}$ refers to the position of the prey at time t, $X_p(t)$ is the position of the wolf at time t, and D implies to the distance between the wolf and the prey. A and C are vectors of coefficients that are defined as equation 3 and 4:

$$\vec{A} = 2\vec{a}.\vec{r}_1 - \vec{a} \tag{4}$$

$$\vec{C} = 2.\vec{r}_2 \tag{5}$$

Where a is a variable, whose value decreases linearly from 2 to 0, r_1 and r_2 are random values [63].

The gray wolves attack on prey during the hunting phase, which is led by the alpha. Sometimes beta and delta wolves participate in the hunt. This process can also come to mathematical relation, within an assumption that assumes alpha, beta, and delta wolves have better knowledge of the potential location of the prey. Therefore, the obtained solutions for selection are saved and the rest of the search agents update their position according to the position of the best solutions [43,50]. The following equations quantify this process:

$$\vec{D}_\alpha = |\vec{C}_1.\vec{X}_\alpha - \vec{X}|$$

$$\vec{D}_\beta = |\vec{C}_2.\vec{X}_\beta - \vec{X}| \tag{6}$$

$$\vec{D}_\delta = |\vec{C}_3.\vec{X}_\delta - \vec{X}|$$

$$\vec{X}_1 = \vec{X}_\alpha - \vec{A}_1.\vec{D}_\alpha$$

$$\vec{X}_2 = \vec{X}_\beta - \vec{A}_1.\vec{D}_\beta \tag{7}$$

$$\vec{X}_3 = \vec{X}_\delta - \vec{A}_1.\vec{D}_\delta$$

$$\vec{X}_{(t+1)} = \frac{\vec{X}_1 + \vec{X}_2 + \vec{X}_3}{3} \tag{8}$$

Through the searching for prey, the wolves move apart to search different points of the solution space. Hence, a random vector with a value greater than 1 or less than -1 represents the mathematical model in this regard. When the prey stops, gray wolves attack and the hunting ends. To model the attack on the prey the (a) parameter is reduced [43].

4. Results and discussion
4.1. GMPI maps

The main data used in this study is stream sediment data. In addition, the objective is to determine the area of porphyry copper mineralization potential in the study area based on the stream sediment data. Based on the data, some elements have a strong correlation that were selected for this study. The Au and Cu as the main mineralization elements were selected. Also the

Mo, As, Pb and Zn have good correlation with mineralization as trace and paragenesis elements.

For this purpose, the GMPI maps of geochemical signature were created. In the first, the GMPI for Cu-Au, Mo-As, and Pb-Zn based on the eq.1, and then based on the [34] GMPI map for copper porphyry were prepared and presented in Figure 3. In these maps, the value of the mineralization index is shown between 0 and 1and

indicates the possibility of mineralization. Values with mineralization potential are marked with a red spectrum color (yellow to red) on the generated maps. Thus, the more toward red, the greater the mineralization potential. The main challenge is considering a value as an anomaly. There are several methods for determining the anomaly separation limit, each with its own advantages and disadvantages.
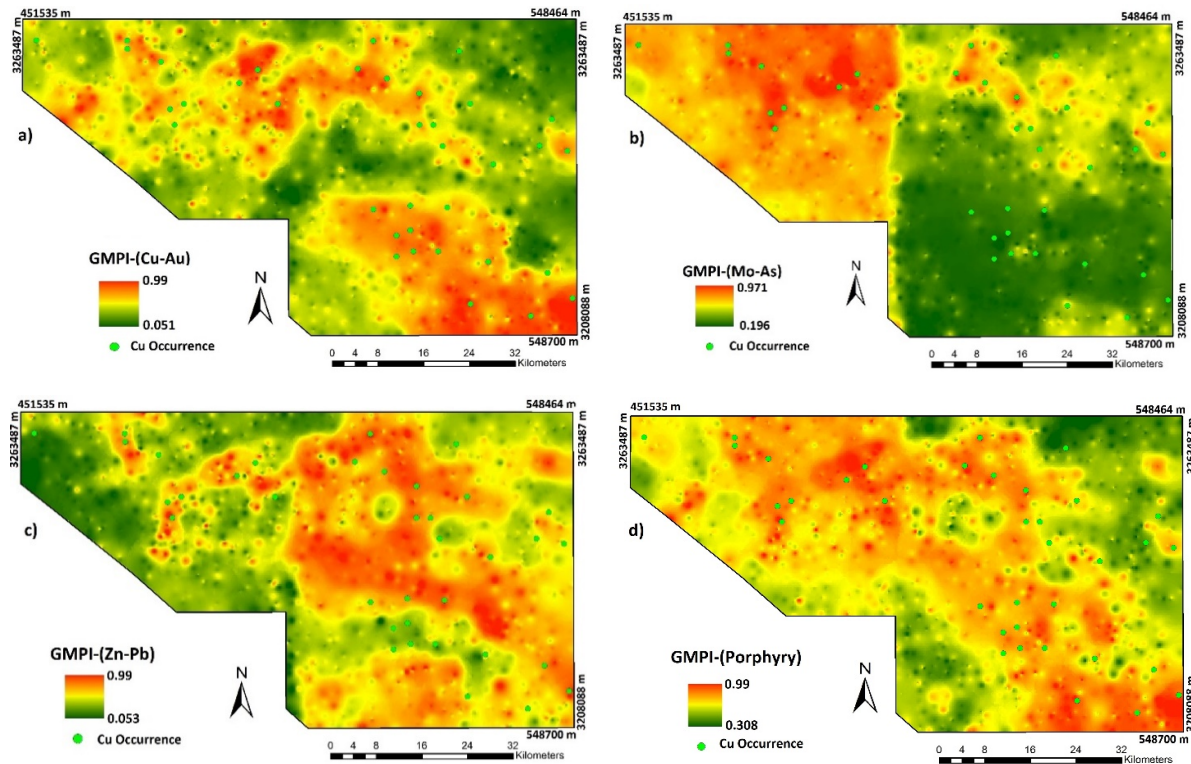

Figure 3. GMPI maps of Cu-Au (a), Mo-As (b), Zn-Pb (c), and Porphyry (d) in study area.

4.2. Anomaly Determination

This paper attempts to place an appropriate boundary on the GMPI map to properly identify high potential mineralized zones. Fractal is one of the most powerful and widely used techniques in geochemical data analysis. Therefore, in this research, fractal methods were first used with Concentration-Area (C-A) technique to classify GMPI maps and the generated maps were classified (Figure 4).

Obviously, it would be an arduous task to consider which of these limits as optimized one and this is where optimization algorithm, gray wolf optimization particularly, changes the story, makes the selection process easy and eliminate any

misinterpretation. The Gray wolf algorithm applied on GMPI maps within the MATLAB software. Running the algorithm needs to define some specific parameters including data range, iteration number, and gray wolf number. For this study, the number of iteration and wolf's pack size were set at 100 and 50, respectively. Equation (9) implies to cost function used in this investigation:

$$f(x) = \sum_{i=1}^{n} |x - x_i| \qquad (9)$$

Where x =optimized separation value, x_i= fractal limit values and the spectrum' upper bound, and n= number of fractal limits. The optimal point occurs where the cost function possesses the lowest possible value (Figure 5).
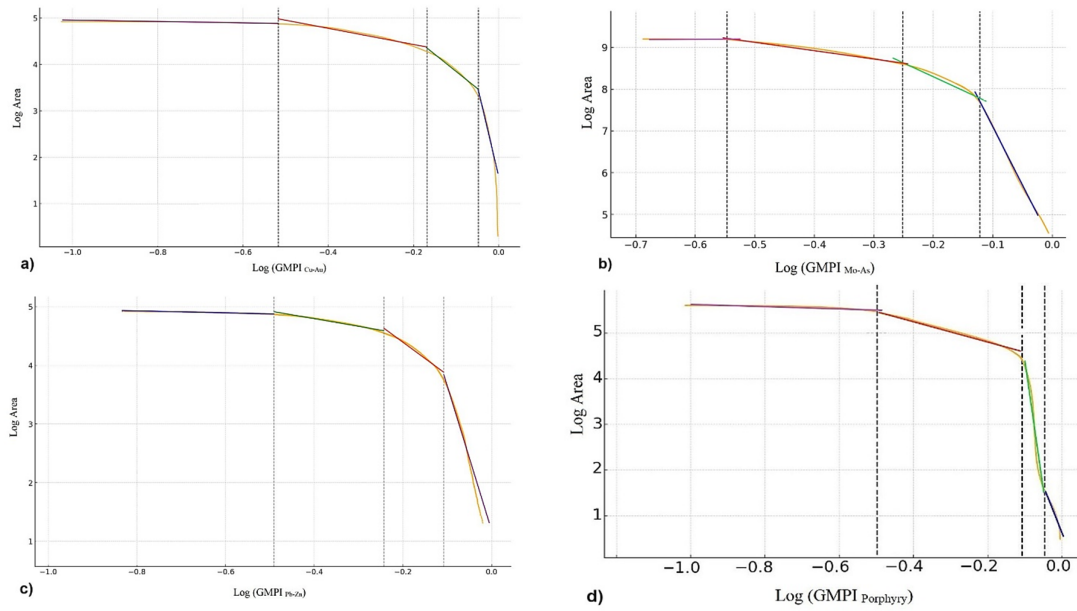
Figure 4. Fractal log(C-A) plots of Cu-Au (a), Mo-As (b), Zn-Pb (c), and Porphyry (d)
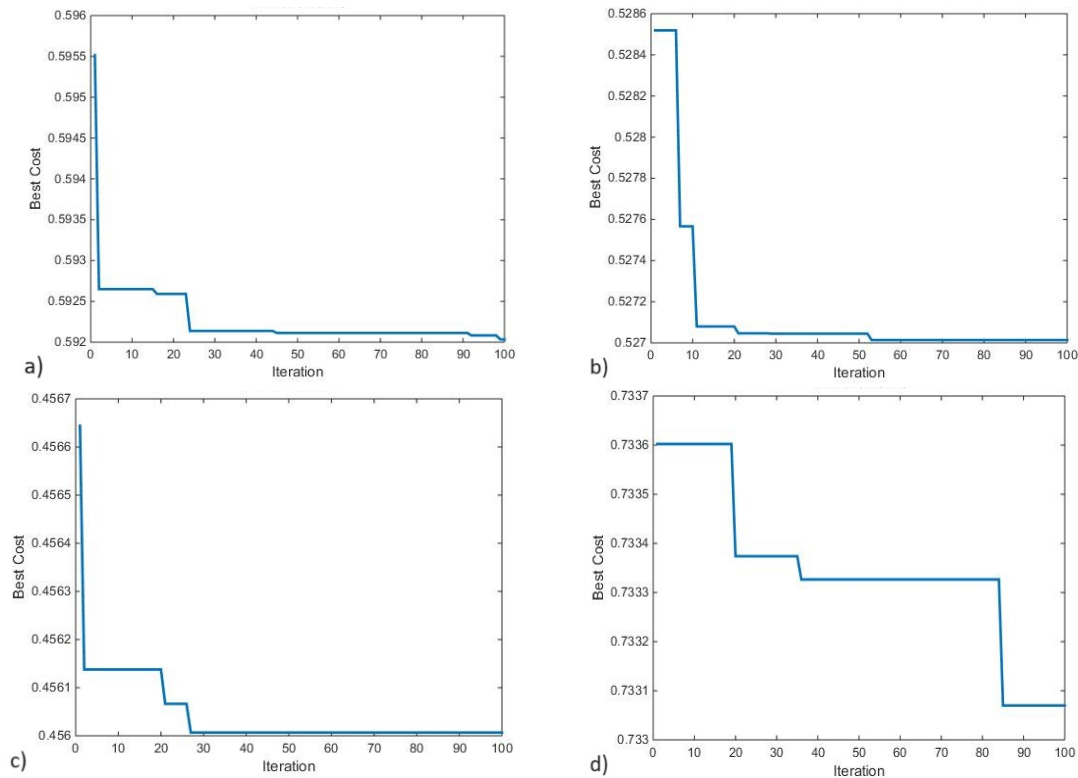

Figure 5. the trend WGO algorithm for GMPIs, a) Cu-Au, b) Mo-As, c) Pb-Zn, and d) Porphyry

The GMPI map of Cu-Au is divided into three classes according to the fractal C-A method. Therefore, we have three classification limits: L1=0.304, L2=0.677, and L3=0.896. Based on these values, an anomaly map was created for each boundary by green color (Figure 6. a, b, and c). This makes it difficult to identify a particular group

as an anomaly and can lead to misinterpretation. It is therefore not possible to comment accurately on the separation of anomalies from background. GWO algorithm is powerful and useful tools to overcome this difficulty. The optimal separation limit of 0.737 was obtained by applying the GWO algorithm (Figure 6. d).
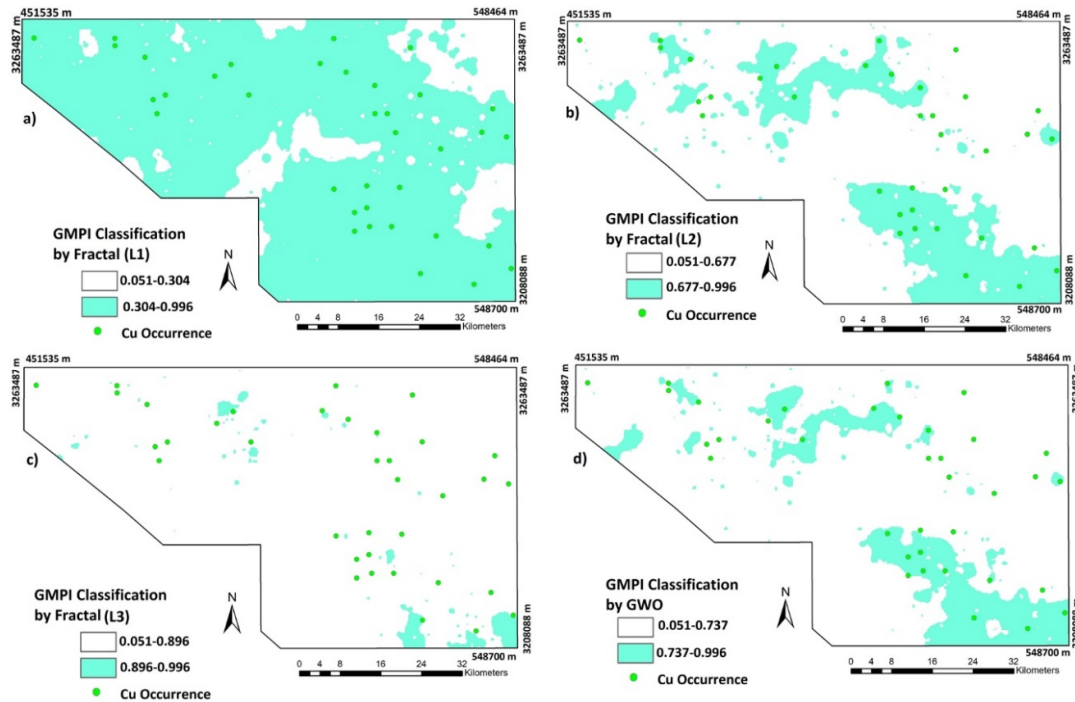
Figure 6. GMPI map classification by fractal: a) L1, b) L2, c) L3, and d) optimal boundary by GWO for Cu-Au

As mentioned above, the GMPI map of Mo-As was prepared because it is an indicator of porphyry copper mineralization. Classification of GMPI (Mo-As) map was done using fractal methods (C-A). Based on the fractal results, the map values were classified into four population, resulting in three separation limits: L1=0.284, L2=0.56 and L3=0.755. Anomaly maps were generated using the obtained separation limits (Figure 7 a, b, and c) and anomalies were colored green. In the following, based on the results of the GWO algorithm, the optimal separation limit has been determined, its value is 0.693. This is how the classified GMPI map of Mo-As with its boundary was created (Figure 7 d).

The GMPI of Pb-Zn has been mapped as another indicator of porphyry copper deposits. For this reason, its classification was carried out based on the fractal C-A methods. Based on the fractal results, this map was divided into four groups and their separation limits were obtained, the values of which are L1=0.323, L2=0.571 and L3=0.779. Anomaly maps based on the obtained separation limits are presented in Figure 8. a, b and c. Using

the GWO algorithm, the optimal value for separating the anomaly from the background was found to be 0.671, and GMPI anomaly map was generated based on this (Figure 8. d). On these maps (Figure 6) the anomaly area is marked by a green color.

As mentioned, a porphyry GMPI map has been produced taking into account the effects of all the above index elements. Now we need to identify the anomaly areas based on the map we have prepared (Fig3.d). Therefore, the classification of the map was done based on the fractal method, and based on the results, three limits for the separation of anomaly values were identified, which are 0.308, 0.754 and 0.896. The anomaly maps were generated and the anomaly boundary was determined in each of them (Fig9.a, b and c). Then, through the application of the GWO algorithm, the optimal limit of the separation of the anomalies was determined, which is 0.839, and its map was created (Figure 9.d). The boundary of the anomaly is marked and the anomalous areas are highlighted in green on the prepared map.
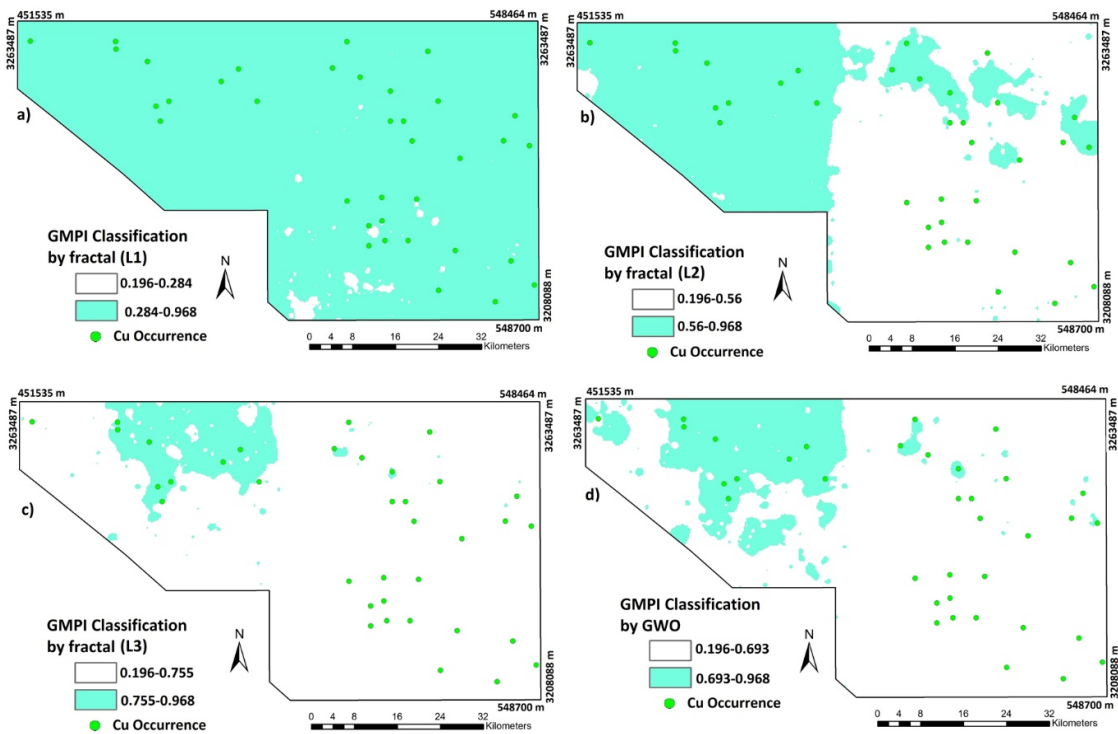
Figure 7. GMPI map classification by fractal: a) L1, b) L2, c) L3, and d) optimal boundary by GWO for Mo-As
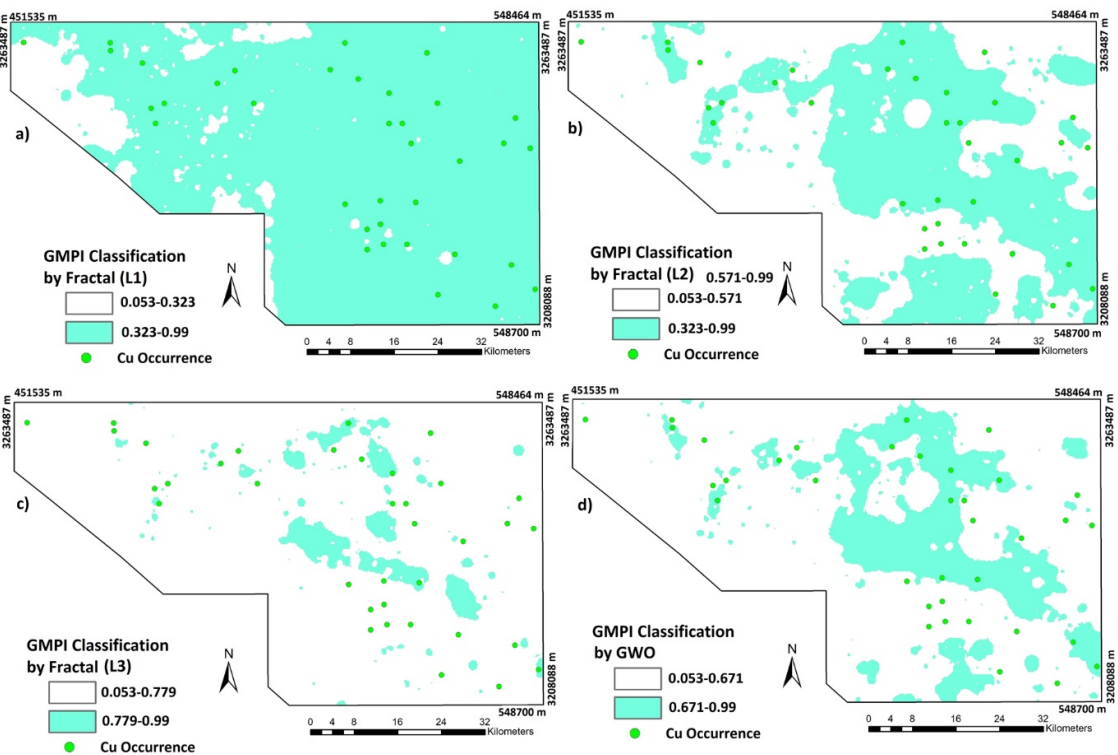

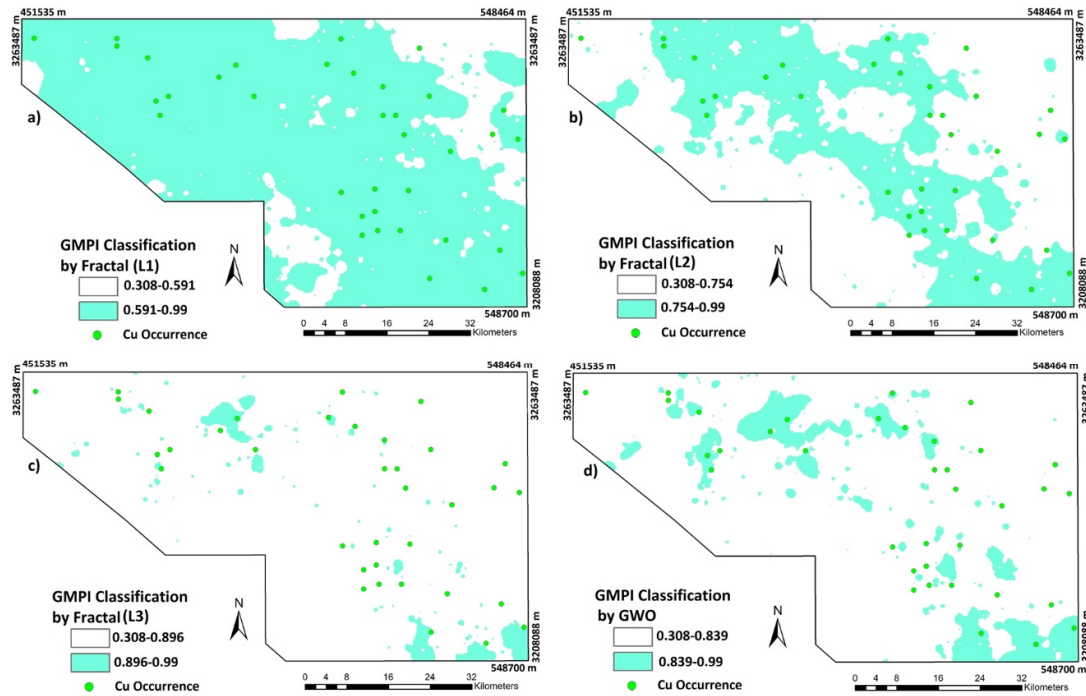**Figure 8. GMPI map classification by fractal: a) L1, b) L2, c) L3, and d) optimal boundary by GWO for Pb-Zn**

1172

Figure 9. Porphyry GMPI map classification by fractal: a) L1, b) L2, c) L3, and d) optimal boundary by GWO

5. Validation by Risk analysis

In this research we used fractal method and GWO algorithm for detection of anomalous values from prepared GMPI maps. Using these methods, anomaly classification was performed and anomaly boundaries were established with the obtained limits. However, which limit to choose and based on which limit the anomaly boundary should be determined is the main discussion and challenge here. The fractal method tends to produce multiple classes, making the decision about the anomaly boundary difficult and controversial. It is a challenge to select each of the boundaries obtained by the fractal method. This is because a very large area is defined as anomaly and target area if we choose the initial limits (low values). If the target area is large, a lot of time and cost has to be spent on exploration, which is virtually impossible for technical and economic reasons. The target area becomes very small and the possibility of losing potential areas increases if we choose the upper limits (higher values). Therefore, as a result, the risk of an exploratory operation is increased. One obvious difference, however, is that the use of GWO produces only two categories; anomaly and background. This leads to the avoidance of relying on the judgment of experts.

The location of known deposits was used to further investigation and validation of the results. The area covered and the number of the detected

Cu occurrences were calculated by selecting different boundaries. As mentioned, the general rule in exploration studies is that the more deposits you can find in a smaller area, the better it is. Therefore, the validation was done according to this point. We introduce the risk of boundary selection by detection of Cu occurrence and covered area per each selected limit. The amount of risk associated with each of the selected limits was then calculated using Equation 10.

$$Risk = \frac{N}{S} \qquad (10)$$

Where, N represents the percentage of known Cu occurrence, and S is the percentage of area covered.

The reliability index was obtained based on the eq.10, as defined in equation 11:

Reliability index=1-Risk   (11)

The value of this index, ranges between [0-1], with the values closer to one, the better. In other words, it is more efficient because it has identified more deposits in a smaller area. A risk analysis was done on the anomaly separation limits and a reliability index was calculated for the GMPI maps in used (Figure 10).
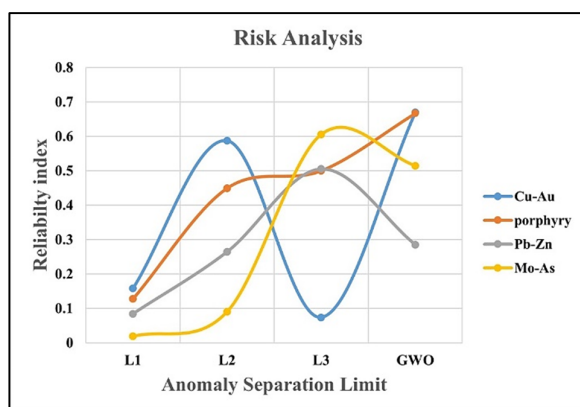
Figure 10. The results of risk analysis

The reliability index of the Cu-Au and porphyry GMPI maps for the GWO anomaly boundary is higher than that of the fractal boundaries, meaning that the efficiency of the algorithm is much better in determining the anomaly of these maps. As mentioned before, the porphyry GMPI map is a combination of other GMPI maps, based on which the target zone is introduced. The reliability index of the porphyry GMPI is 0.13, 0.45, and 0.5 for L1, L2, and L3, respectively, by fractal methods, while this value is 0.67 for the GWO limit. Thus, the choice of the GWO's limit will have the effect that more deposits will be detected in less area.

6. Conclusions

This study aimed to address challenges of geochemical anomaly detection by introducing the Grey Wolf Optimizer (GWO) algorithm as a novel approach for binary geochemical anomaly detection and separation in stream sediment data. While the initial application of fractal analysis on GMPI distributions resulted in several anomalous classes, making limit selection difficult, the GWO algorithm provided a unique and optimized value for each distribution.

Risk analysis, performed via a reliability index calculation, demonstrated the superiority of the GWO-derived limit compared to those obtained using fractal methods. The reliability index of the porphyry GMPI, as the main criteria for detecting target areas, is 0.67 by selecting the GWO boundary, while this value is 0.13, 0.45, and 0.5 for L1, L2, and L3, respectively, for fractal methods. These results suggest that the GWO algorithm can be a valuable tool for anomaly detection and optimal threshold selection in geochemical exploration studies.

This framework is still under development and requires further refinement and application by geoscientists to solve problems in mineral exploration, environmental investigations, and remote sensing. Given the continuous advancements in swarm intelligence algorithms, future research exploring the application of alternative algorithms for anomaly detection is highly recommended.

References

[1]. Mostafaei, K., & Ramazi, H. (2019). Mineral resource estimation using a combination of drilling and IP-Rs data using statistical and cokriging methods. *Bulletin of the mineral research and exploration*, *160*(160), 177-195.

[2]. Mostafaei, K., & Kianpour, M. (2022). Application of Magnetometry in Manto-type Copper Deposit Exploration, Case study: Meyami, Iran. *Rudarsko-geološko-naftni zbornik*, *37*(5), 1-14.

[3]. Mohammadi, N. M., Hezarkhani, A., Saljooghi, B. S. (2016). Separation of a geochemical anomaly from background by fractal and U-statistic methods, a case study: Khooni district, Central Iran. *Geochemistry*, *76*(4), 491-499.

[4]. Yilmaz, H., Yousefi, M., Parsa, M., Sonmez, F. N., & Maghsoodi, A. (2019). Singularity mapping of bulk leach extractable gold and− 80# stream sediment geochemical data in recognition of gold and base metal mineralization footprints in Biga Peninsula South, Turkey. *Journal of African Earth Sciences*, *153*, 156-172.

[5]. Ghasemzadeh, S., Maghsoudi, A., Yousefi, M., & Mihalasky, M. J. (2022). Recognition and incorporation of mineralization-efficient fault systems to produce a strengthened anisotropic geochemical singularity. *Journal of Geochemical Exploration*, *235*, 106967.

[6]. Yousefi, M., Barak, S., Salimi, A., & Yousefi, S. (2023). Should Geochemical Indicators Be Integrated to Produce Enhanced Signatures of Mineral Deposits? A Discussion with Regard to Exploration Scale. *Journal of Mining and Environment*, *14*(3), 1011-1018. doi: 10.22044/jme.2023.13160.2398

[7]. Seyedrahimi-Niaraq, M., Shokri, N., & Lotfibakhsh, A. (2023). Improving the method of U-spatial statistics by modeling the enrichment index of stream sediments for the purpose of introducing geochemical anomalous areas of epithermal gold type mineralization. *Journal of Mining Engineering, 18*(59), 15-30.

[8]. Chen, J., Yousefi, M., Zhao, Y., Zhang, C., Zhang, S., Mao, Z., & Han, R. (2019). Modelling ore-forming processes through a cosine similarity measure: Improved targeting of porphyry copper deposits in the Manzhouli belt, China. *Ore Geology Reviews, 107*, 108-118.

[9]. Yousefi, M., & Hronsky, J. M. (2023). Translation of the function of hydrothermal mineralization-related focused fluid flux into a mappable exploration criterion

for mineral exploration targeting. *Applied Geochemistry, 149*, 105561.

[10] Seyedrahimi-Niaraq, M., & Mahdiyanfar, H. (2021). Introducing a new approach of geochemical anomaly intensity index (GAII) for increasing the probability of exploration of shear zone gold mineralization. *Geochemistry, 81*(4), 125830.

[10]. Reimann, C., Filzmoser, P., Hron, K., Kynčlová, P., Garrett, R. G. (2017). A new method for correlation analysis of compositional (environmental) data–a worked example. *Science of the Total Environment, 607*, 965-971.

[11]. Yousefi, M., Yousefi, S., & Kamkar Rouhani, A. (2023). Recognition coefficient of spatial geological features, an approach to facilitate criteria weighting for mineral exploration targeting. International Journal of Mining and Geo-Engineering, (), 251-258. doi: 10.22059/ijmge.2023.355380.595037

[12]. Seyedrahimi-Niaraq, M., Mahdiyanfar, H., & Mokhtari, A. R. (2022). Integrating principal component analysis and U-statistics for mapping polluted areas in mining districts. *Journal of Geochemical Exploration, 234*, 106924.

[13]. Cheng, Q., & Li, Q. (2002). A fractal concentration–area method for assigning a color palette for image representation. *Computers & geosciences, 28*(4), 567-575.

[14]. Chen, Y., Lu, L., & Li, X. (2014). Application of continuous restricted Boltzmann machine to identify multivariate geochemical anomaly. *Journal of Geochemical Exploration, 140*, 56-63.

[15]. Abedi, M., Kashani, S. B. M., Norouzi, G. H., & Yousefi, M. (2017). A deposit scale mineral prospectivity analysis: A comparison of various knowledge-driven approaches for porphyry copper targeting in Seridune, Iran. *Journal of African Earth Sciences, 128*, 127-146.

[16]. Rahimi, H., Abedi, M., Yousefi, M., Bahroudi, A., & Elyasi, G. R. (2021). Supervised mineral exploration targeting and the challenges with the selection of deposit and non-deposit sites thereof. *Applied Geochemistry, 128*, 104940.

[17]. Mostafaei, K., Maleki, S., Jodeiri Shokri, B., & Yousefi, M. (2023). Predicting gold grade by using support vector machine and neural network to generate an evidence layer for 3D prospectivity analysis. *International Journal of Mining and Geo-Engineering, 57*(4),435-444.

[18]. Afzal, P., Khakzad, A., Moarefvand, P., Omran, N. R., Esfandiari, B., & Alghalandis, Y. F. (2010). Geochemical anomaly separation by multifractal modeling in Kahang (Gor Gor) porphyry system, Central Iran. *Journal of Geochemical Exploration, 104*(1-2), 34-46.

[19]. Mahdiyanfar, H., & Seyedrahimi-Niaraq, M. (2024). Application of hybrid Wavelet-Fractal approach for denoising and spatial modeling of environmental pollution. *Journal of Mining and Environment.* doi: 10.22044/jme.2024.14197.2643

[20]. Afzal, P., Mirzaei, M., Yousefi, M., Adib, A., Khalajmasoumi, M., Zarifi, A. Z., Yasrebi, A. B. (2016). Delineation of geochemical anomalies based on stream sediment data utilizing fractal modeling and staged factor analysis. *Journal of African Earth Sciences, 119*, 139-149.

[21]. Ghezelbash, R., & Maghsoudi, A. (2018). A hybrid AHP-VIKOR approach for prospectivity modeling of porphyry Cu deposits in the Varzaghan District, NW Iran. *Arabian Journal of Geosciences, 11*, 1-15.

[23]. Ghezelbash, R., Maghsoudi, A., & Carranza, E. J. M. (2020). Optimization of geochemical anomaly detection using a novel genetic K-means clustering (GKMC) algorithm. *Computers & Geosciences, 134*, 104335.

[24]. Aryafar, A., Moeini, H., & Khosravi, V. (2020). CRFA-CRBM: a hybrid technique for anomaly recognition in regional geochemical exploration; case study: Dehsalm area, east of Iran. *International Journal of Mining and Geo-Engineering, 54*(1), 33-38.

[25]. Farhadi, S., Afzal, P., Boveiri Konari, M., Daneshvar Saein, L., & Sadeghi, B. 2022. Combination of Machine Learning Algorithms with Concentration-Area Fractal Method for Soil Geochemical Anomaly Detection in Sediment-Hosted Irankuh Pb-Zn Deposit, *Central Iran. Minerals, 12*(6), 689.

[26]. Mahdiyanfar, H., & Seyedrahimi-Niaraq, M. (2022). Improvement of geochemical prospectivity mapping using power spectrum–area fractal modelling of the multi-element mineralization factor (SAF-MF). *Geochemistry: Exploration, Environment, Analysis, 22*(4), geochem2022-015.

[27]. Heidari, S. M., Afzal, P., & Sadeghi, B. (2024). Molybdenum and gold distribution variances within Iranian copper porphyry deposits. *Journal of Geochemical Exploration, 261*, 107471.

[28]. Pourgholam, M. M., Afzal, P., Adib, A., Rahbar, K., & Gholinejad, M. (2024). Recognition of REEs anomalies using an image Fusion fractal-wavelet model in Tarom metallogenic zone, NW Iran. *Geochemistry, 84*(2), 126093.

[29]. Mostafaei, K., Ramazi, H. (2018). Compiling and verifying 3D models of 2D induced polarization and resistivity data by geostatistical methods. *Acta Geophysica, 66*, 959-971.

[30]. Chen, Y., & Shayilan, A. (2022). Dictionary learning for multivariate geochemical anomaly detection for mineral exploration targeting. *Journal of Geochemical exploration, 235*, 106958.

[31]. Luo, Z., Zuo, R., Xiong, Y., & Zhou, B. (2023). Metallogenic-Factor Variational Autoencoder for Geochemical Anomaly Detection by Ad-Hoc and Post-Hoc Interpretability Algorithms. *Natural Resources Research*, 1-19.

[32]. Chen, Y., & Lu, L. (2023). The Anomaly Detector, Semi-supervised Classifier, and Supervised Classifier Based on K-Nearest Neighbors in Geochemical Anomaly Detection: A Comparative Study. *Mathematical Geosciences*, 1-23.

[33]. Chen, Z., Xiong, Y., Yin, B., Sun, S., & Zuo, R. (2023). Recognizing geochemical patterns related to mineralization using a self-organizing map. *Applied Geochemistry, 151*, 105621.

[34]. Yousefi, M., Kamkar-Rouhani, A., & Carranza, E. J. M. (2012). Geochemical mineralization probability index (GMPI): a new approach to generate enhanced stream sediment geochemical evidential map for increasing probability of success in mineral potential mapping. *Journal of Geochemical Exploration, 115*, 24-35.

[35]. Helba, H. A., El-Makky, A. M., & Khalil, K. I. (2021). Application of the CN fractal model, factor analysis and geochemical mineralization probability index (GMPI) for delineating geochemical anomalies related to a Mn-Fe deposit and associated Cu mineralization in west-central Sinai, Egypt. *Geochemistry: Exploration, Environment, Analysis, 21*(3), geochem2021-031.

[36]. Yousefi, M., & Carranza, E. J. M. (2016). Data-driven index overlay and Boolean logic mineral prospectivity modeling in greenfields exploration. *Natural Resources Research, 25*, 3-18.

[37]. Yousefi, M., Carranza, E. J. M., Kreuzer, O. P., Nykänen, V., Hronsky, J. M., & Mihalasky, M. J. (2021). Data analysis methods for prospectivity modelling as applied to mineral exploration targeting: State-of-the-art and outlook. *Journal of Geochemical Exploration, 229*, 106839.

[38]. Ouchchen, M., Boutaleb, S., Abia, E. H., El Azzab, D., Miftah, A., Dadi, B., & Abioui, M. (2022). Exploration targeting of copper deposits using staged factor analysis, geochemical mineralization prospectivity index, and fractal model (Western Anti-Atlas, Morocco). *Ore Geology Reviews, 143*, 104762.

[39]. Marques, E. D., Castro, C. C., de Assis Barros, R., Lombello, J. C., de Souza Marinho, M., Araújo, J. C. S., & Santos, E. A. (2023). Geochemical mapping by stream sediments of the NW portion of Quadrilátero Ferrífero, Brazil: Application of the exploratory data analysis (EDA) and a proposal for generation of new gold targets in Pitangui gold district. *Journal of Geochemical Exploration, 250*, 107232.

[40]. Derrac, J., García, S., Molina, D., & Herrera, F. (2011). A practical tutorial on the use of nonparametric statistical tests as a methodology for comparing evolutionary and swarm intelligence algorithms. *Swarm and Evolutionary Computation, 1*(1), 3-18.

[41]. Cui, Z. H., and GAO, X. Z. (2012). Theory and applications of swarm intelligence. *Neural Computing and Applications. 21*, 205–206.

[42]. Parpinelli, R. S., & Lopes, H. S. (2011). New inspirations in swarm intelligence: a survey. *International Journal of Bio-Inspired Computation, 3*(1), 1-16.

[43]. Leboucher, C., Chelouah, R., Siarry, P., Le Ménec, S. (2012). A swarm intelligence method combined to evolutionary game theory applied to the resources allocation problem. *International Journal of Swarm Intelligence Research (IJSIR), 3*(2), 20-38.

[44]. Zhang, Z., Long, K., Wang, J., Dressler, F. (2013). On swarm intelligence inspired self-organized networking: its bionic mechanisms, designing principles and optimization approaches. *IEEE Communications Surveys & Tutorials, 16*(1), 513-537.

[45]. Li, S. Y., Wang, S. M., Wang, P. F., Su, X. L., Zhang, X. S., Dong, Z. H. (2018). An improved grey wolf optimizer algorithm for the inversion of geoelectrical data. *Acta Geophysica, 66*(4), 607-621.

[46]. Nadimi-Shahraki, M. H., Taghian, S., Mirjalili, S. (2021). An improved grey wolf optimizer for solving engineering problems. *Expert Systems with Applications, 166*, 113917.

[47]. Otair, M., Ibrahim, O. T., Abualigah, L., Altalhi, M., & Sumari, P. (2022). An enhanced grey wolf optimizer-based particle swarm optimizer for intrusion detection system in wireless sensor networks. *Wireless Networks, 28*(2), 721-744.

[48]. Almazini, H. F., Ku-Mahamud, K. R., & Almazini, H. (2023). Heuristic Initialization Using Grey Wolf Optimizer Algorithm for Feature Selection in Intrusion Detection. *International Journal of Intelligent Engineering & Systems, 16*(1), 410-418.

[49]. Li, S., Mao, J., & Li, Z. (2023). An EEMD-SVD method based on gray wolf optimization algorithm for lidar signal noise reduction. *International Journal of Remote Sensing, 44*(17), 5448-5472.

[50]. Mostafaei, K., Kianpour, M. N., & Yousefi, M. (2024). Delineation of Gold Exploration Targets based on Prospectivity Models through an Optimization Algorithm. *Journal of Mining and Environment, 15*(2), 597-611.

[51]. Hezarkhani, A. (2006). Mineralogy and fluid inclusion investigations in the Reagan Porphyry System, Iran, the path to an uneconomic porphyry copper deposit. *Journal of Asian Earth Sciences, 27*(5), 598-612.

[52]. Azizi, H., Stern, R. J., Topuz, G., Asahara, Y., & Moghadam, H. S. (2019). Late Paleocene adakitic granitoid from NW Iran and comparison with adakites

in the NE Turkey: Adakitic melt generation in normal continental crust. *Lithos, 346*, 105151.

[53]. Moinevaziri, H., Akbarpour, A., & Azizi, H. (2015). Mesozoic magmatism in the northwestern Sanandaj–Sirjan zone as an evidence for active continental margin. *Arabian journal of geosciences, 8*, 3077-3088.

[54]. Shafiei, B., Haschke, M., & Shahabpour, J. (2009). Recycling of orogenic arc crust triggers porphyry Cu mineralization in Kerman Cenozoic arc rocks, southeastern Iran. *Mineralium Deposita, 44*, 265-283.

[55]. Dorani, M., & Moradian, A. (2007). Geochemical and tectonomagmatic investigation of gabbros in southwest of Shahr-Babak, Kerman Province. *Iran Soc Cryst Mineral, 86*, 193-210.

[56]. Hezarkhani, A. (2006). Hydrothermal evolution of the Sar-Cheshmeh porphyry Cu–Mo deposit, Iran: evidence from fluid inclusions. *Journal of Asian Earth Sciences, 28*(4-6), 409-422.

[57]. Hezarkhani, A. (2009). Hydrothermal fluid geochemistry at the Chah-Firuzeh porphyry copper deposit, Iran: Evidence from fluid inclusions. *Journal of Geochemical Exploration, 101*(3), 254-264.

[58]. Afzal, P., Khakzad, A., Moarefvand, P., Omran, N. R., Esfandiari, B., & Alghalandis, Y. F. (2010). Geochemical anomaly separation by multifractal modeling in Kahang (Gor Gor) porphyry system, Central Iran. *Journal of Geochemical Exploration, 104*(1-2), 34-46.

[60]. Sepahi, A. A., Ghoreishvandi, H., Maanijou, M., Maruoka, T., Vahidpour, H., 2020. Geochemical description and sulfur isotope data for Shahrak intrusive body and related Fe-mineralization (east Takab), northwest Iran. *Island Arc, 29*(1), e12367.

[61]. Geological survey of Iran, 1972. www.ngdi.ir

[62]. Yousefi, M., Kamkar-Rouhani, A., & Carranza, E. J. M. (2014). Application of staged factor analysis and logistic function to create a fuzzy stream sediment geochemical evidence layer for mineral prospectivity mapping. *Geochemistry: Exploration, Environment, Analysis, 14*(1), 45-58.

[63]. Mirjalili, Seyedali, Seyed Mohammad Mirjalili, and Andrew Lewis. (2014). Grey wolf optimizer. *Advances in engineering software 69*: 46-61.

بهبود نتایج مدل فرکتالی شاخص احتمال کانی‌سازی ژئوشیمیایی با استفاده از الگوریتم گرگ خاکستری در داده‌های رسوبات آبراهه‌ای منطقه ساردویه – بافت

کامران مصطفائی[۱]، محمد نبی کیانپور[۲]*، مهیار یوسفی[۳] و میثم سالکی[۲]

۱- گروه مهندسی معدن، دانشکده مهندسی، دانشگاه کردستان، سنندج، ایران

۲- دانشکده مهندسی مواد و منابع معدنی، پردیس مهندسی، دانشگاه سانیس مالزی، مالزی

۳- دانشکده مهندسی، دانشگاه ملایر، ملایر، ایران

* نویسنده مسئول مکاتبات: K.mostafaei@uok.ac.ir

چکیده:

تفکیک آئومالی‌های ژئوشـیمیایی از زمینه همواره یک چالش اسـت زیرا الگوهای پراکندگی عناصـر تحت تاثیر عوامل مختلف زمین‌شـناسـی قرار گرفته که از یک ناحیه تا ناحیه‌ای دیگر متفاوت اسـت. معمولا از روش‌های آماری و فرکتالی برای تشـخیص آنومالی‌ها اسـتفاده می‌شـود که در تعیین حد آسـتانه بهینه دچار چالش می‌باشند. این مطالعه الگوریتم گرگ خاکستری را به عنوان یک رویکرد جدید در تعیین حد بهینه آنومالی و زمینه پیشنهاد می‌کند. از داده‌های ژئوشیمی رسوبات آبراهه‌ای منطقه ساردوئیه-بافت در جنوب شرق ایران که دارای کانی‌سازی مس می‌باشد به عنوان مطالعه موردی جهت تجزیه و تحلیل اسـتفاده شد. ابتدا شاخص احتمال کانی‌سازی ژئوشیمیایی برای مس-طلا، مولیبدن-آرسنیک سرب-روی و پورفیری محاسبه شده و نقشه آنها تهیه شد. در ادامه از روش‌های فرکتالی برای تعیین جوامع آنومالی در هر کدام از نقشـه‌های تهیه شده اسـتفاده شـد. سپس از الگوریتم گرگ خاکستری برای تعیین حدهای بهینه نتایج فرکتالی اسـتفاده شـد. آنالیز ریسـک براساس نسبت تعداد اندیس شناسایی شده نسبت به مساحت تحت پوشش انجام شده و نتایج نشان داد که حد بدست آمده از روش الگوریتم گرگ خاکسـتری در مقایسـه با سـایر حدهای بدسـت آمده از روش فرکتال قابلیت اطمینان بیشـتری دارد. برای شاخص احتمال کانی‌سازی ژئوشیمیایی پورفیری مقادیر شـاخص قابلیت اطمینان برای حدهای فرکتالی به ترتیب عبارتند از : ۰/۱۲۷، ۰/۴۴ و ۰/۵ می‌باشـد این مقدار برای حد بدسـت آمده از الگوریتم گرگ خاکستری ۰/۶۶ می‌باشـد. همچنین نتایج بدست آمده برای نقشه مس-طلا نشـان می‌دهد که حد بدسـت آمده از الگوریتم گرگ خاکسـتری نتایج بهتری دارد. بنابراین نتایج نشان می‌دهد که الگوریتم گرگ خاکسـتری در تعیین حد بهینه تفکیک آنومالی از زمینه در نقشـه‌های شـاخص احتمال کانی‌سـازی ژئوشـیمیایی عملکرد موفقی داشته است.

کلمات کلیدی: داده‌های ژئوشیمیایی، رسوبات آبراهه‌ای، الگوریتم بهینه‌ساز گرگ خاکستری، تعیین آنومالی.